Investigation of Hydrogen Leaks from Double Ferrule Fittings

Tianze Wang[a], Fuyuan Yang*[a, b], Xintao Deng[a], Jian Dang[a], Yangyang Li[a], Song Hu[a] and Minggao Ouyang[a]

[a] School of Vehicle and Mobility, State Key Laboratory of Automotive Safety and Energy, Tsinghua University, Beijing 100084, China

[b] Collaborative Innovation Center of Electric Vehicles in Beijing, Beijing 100081, China

Abstract

The use of hydrogen is expected to increase rapidly in the future. Leakage of hydrogen pipework are the main forms of safety problems in hydrogen utilization. In this paper, a numerical model of hydrogen leakage and diffusion in pipe joints was established. The Schlieren + high-speed camera is used in experiments to observe the leakage of hydrogen in the pipe joints. In addition, the shape and size of the scratches in the tube were statistically analyzed. Finally, the leakage characteristics of double ferrule joints with scratches are experimentally analyzed. For the two scratch sizes, the critical pressure values for the vortex transition are 0.2 MPa and 0.03 MPa. Through our experimental process, some practical experience and suggestions are given.

Keywords：

Hydrogen safety; Numerical simulation; Double Ferrule Fittings; hydrogen leakage

1. Introduction

Hydrogen has received extensive attention in recent years because of its clean, efficient, and renewable characteristics. However, considering the characteristics of hydrogen, it is difficult to maintain safety in production, storage, transportation, and utilization. Currently, high-pressure storage of hydrogen is still the most economical way. Hydrogen must operate in a safe and reliable environment, which limits the equipment and pipeworks in contact with hydrogen to meet sealing conditions to avoid leakage, fire, or even explosion. The initial manifestation of all hydrogen safety incidents is leakage and diffusion. Compared with natural gas, hydrogen is more prone to leakage and diffusion. This is because hydrogen has the smallest molecular volume and is easier to escape in small gaps.

After hydrogen leaks, jets with larger Froude numbers are momentum-controlled jets; while jets with lower Froude numbers have a strong buoyancy effect. When hydrogen leaks at subsonic speed, G. Jirka used the integral model to explore the gas diffusion and movement process[1-2]. J.S.

Kim et al. observed the buoyant jet trajectory through shadow technology, and analyzed the buoyant jet trajectory through an integrated model to obtain an approximate formula describing its shape, and gave the horizontal and vertical lengths corresponding to the critical ignition concentration[3]. The jet integral method is achieved by using the boundary layer properties of the flow and integrating all terms of the turbulent Reynolds equation of motion that control the entire cross-section. When hydrogen leaks under a supersonic speed, the "Notional nozzle" model is used to simulate the law of diffusion[4]. The method is to assume that the gas flow exits from an "equivalent" outlet different from the actual leakage outlet, and the pressure of the airflow at the notional nozzle outlet is equal to the atmospheric pressure.

If a hydrogen jet is ignited, a jet flame will be formed, which is a very harmful scenario. Schefer et al. measured and characterized the size and radiation characteristics of a large vertical hydrogen jet flame. The maximum pressure used in the study reached 41.3 MPa, which is usually the internal pressure of the hydrogen storage vessel. Under this pressure, the fluid flowing from the nozzle is classified as an under-expanded jet. After being injected into the atmosphere, the hydrogen stream will further expand and accelerate to form a supersonic jet. The authors studied high-pressure jets up to 413 bar (6000 psi) to verify the application of correlations and scaling laws based on lower-pressure subsonic and choked-flow jet flames[5].

There is a risk of spontaneous ignition when hydrogen leaks continuously. Especially when the leak occurs inside the tube[6-7], in a complex environment[8-9], triggering the discharge of charged particles[10-12], etc. This is due to the extremely low minimum ignition energy (MIE) of hydrogen[13]. The well-recognized theory of hydrogen spontaneous ignition includes reverse Joule-Thomson effect[14-15], electrostatic ignition[10, 12], diffusion ignition[7, 16], hot surface ignition[17-19] and mechanical friction and impact[20], etc. For any accident caused by the spontaneous combustion of hydrogen, the potential spontaneous combustion reason is complicated, because it is often the result of the superposition of multiple theories. Khashayar Nasrifar [14] predicted the inverse Joule-Thomson coefficient μ_{J-T}, giving the critical point temperature of μ_{J-T} as 195K. When the gas below 195 K undergoes a throttling effect, the gas flow temperature will increase. Electrostatic ignition is often cited as the most likely cause of unexplained ignitions of hydrogen. The most common reason for particles with high potential is the lack of a path to the ground[11]. The cause of diffusion ignition is the interaction of shock waves caused by high-speed

jets, and finally, a high-temperature zone is formed to ignite the mixture[16, 21]. It was shown that when hydrogen is released into the slim tube with a minimum release pressure of 3.8 MPa, diffusion ignition will inevitably occur[22].

This paper focuses on the double ferrule joint used in the hydrogen pipework and presents the diffusion form of the double ferrule joint. The schlieren and high-speed camera is used to observe the hydrogen diffusion morphology. The morphology defects were observed by scanning electron microscope (SEM). Further, the commercial computational fluid dynamics (CFD) software STAR-CCM+ V13.04 produced by CD-adapco was used to simulate the diffusion form.

2. Numerical models

Conservation equations

The conservation equations of fluid dynamics are as follows, all the control equations are implemented on STAR CCM+ solver, for the continuity equation, it is defined as:

$$\frac{\partial \overline{\rho}}{\partial t} + \frac{\partial \overline{\rho}\tilde{u}_j}{\partial x_j} = 0 .$$ (1)

Where ρ and u is density and continuum velocity. The conservation of momentum is defined as:

$$\frac{\partial \overline{\rho}\tilde{u}_i}{\partial t} + \frac{\partial \overline{\rho}\tilde{u}_i\tilde{u}_j}{\partial x_j} = -\frac{\partial \overline{p}}{\partial x_i} + \frac{\partial}{\partial x_j}(v+v_t)\left(\frac{\partial \tilde{u}_i}{\partial x_j} + \frac{\partial \tilde{u}_j}{\partial x_i} - \frac{2}{3}\frac{\partial \tilde{u}_k}{\partial x_k}\delta_{ij}\right) + \overline{\rho}g_i .$$ (2)

Where the v is dynamic viscosity, δ_{ij} is the Kronecker symbol. The conservation of energy is defined as:

$$\frac{\partial \overline{\rho}\tilde{E}}{\partial t} + \frac{\partial}{\partial x_j}(\tilde{u}_j(\overline{\rho}\tilde{E}+\overline{p})) = \frac{\partial}{\partial x_j}\left[\left(k+\frac{v_t c_p}{Pr_t}\right)\frac{\partial \tilde{T}}{\partial x_j} - \sum_m \tilde{h}_m(-(\rho D+\frac{v_t}{Sc_t})\frac{\partial \tilde{Y}_m}{\partial x_j}) + \tilde{u}_i(v+v_t)\left(\frac{\partial \tilde{u}_i}{\partial x_j} + \frac{\partial \tilde{u}_j}{\partial x_i} - \frac{2}{3}\frac{\partial \tilde{u}_k}{\partial x_k}\delta_{ij}\right)\right] + S_E$$

. (3)

Where the E is the total energy, Pr is the turbulent Prandtl number, Sc is the Schmidt number, h_m is the enthalpy of species m, Y_m is the mass fraction of species m, and S_E is the source term. The conservation of species is defined as:

$$\frac{\partial \overline{\rho}\tilde{Y}_m}{\partial t} + \frac{\partial \overline{\rho}\tilde{u}_j\tilde{Y}_m}{\partial x_j} = \frac{\partial}{\partial x_j}\left[(\rho D+\frac{v_t}{Sc_t})\frac{\partial \tilde{Y}_m}{\partial x_j}\right] + R_m .$$ (4)

Where, D is the molecular diffusivity, and R_m is source term.

Turbulence models

The three most common turbulence models are Reynolds-Averaged Navier-Stokes turbulence models (RANS), Large Eddy Simulation (LES), and Detached Eddy Simulation (DES), all of which have been integrated into STAR CCM+. The RANS decompose each solution variable in the instantaneous Navier-Stokes equation into its average value and its fluctuation components:

$$\phi = \overline{\phi} + \phi^{'} . \tag{5}$$

Where Φ represents velocity components, pressure, energy, or species concentration.

This study will use the Realizable Two-Layer K-ε model attached to the RANS model to simulate turbulence. The Realizable Two-Layer K-ε model combines the Realizable K-ε model with the Two-Layer approach. Compared to standard K-ε, the model critical coefficient C_{μ} in Realizable K-ε Two-Layer is expressed as a function of mean flow and turbulence properties, rather than assumed to be constant[23]. And the Two-Layer Approach allows the K-ε model to be applied in the viscous-affected layer (including the viscous sub-layer and the buffer layer)[24].

When simulating real flow scenes (especially the flow dominated by buoyancy with low Reynolds number), the K-ε model used in our research has shown good performance in many studies[25-27]. This is the reason why the K-ε model is used in this research because the K-ε model is more suitable for the turbulent flow dominated by buoyancy in our research.

Boundary conditions

The temperature of the hydrogen leaking from the pipework is 273 K, the initial temperature of the air in the environment is 293 K, and the ambient temperature is 20 °C higher than the hydrogen temperature. Before the leak occurred, the calculation domain was initialized to air (containing 29% oxygen and 71% nitrogen). This difference is used to study the temperature change in the process of hydrogen leakage and diffusion. The mass flow range of leaking hydrogen is 1-5 SLPM. The pipe was initially filled in with hydrogen. In the simulation, the composition of air is 20.7% oxygen and 79.3% nitrogen (volume fraction). When simulating the continuous leakage of hydrogen, keep the mass flow rate and temperature of hydrogen at a constant value. The initial pressure of the entire calculation domain is set to the ambient pressure. The outlet boundary conditions are set to the same pressure and temperature as in the calculation domain. The non-slip boundary conditions apply to all surfaces.

Geometry and Computational grid

The computational domain encompasses the 316L stainless steel solid fitting and nut, the tube internal region, and the external fluid region. The leakage outlet separates the entire flow gas area, one side is high-purity hydrogen and the other is air. When leakage occurs, hydrogen is released from the leakage outlet into the ambient air. The geometry is shown in **Fig. 1**. The hydrogen leakage will be determined according to the multiple failure modes of the pipe joints. **Fig. 1c** shows the meshing situation. The leakage occurs at very small scratches and the corresponding minimum grid size is 40 μm. There are about 8-10 cells distributed in the width of the scratch, which can ensure the effectiveness of the cell division. When hydrogen leaks into the space, the grid size is mainly according to the calculation load. In our research, the largest cell size is 2000 μm, and the grid size range is set to 40-2000 μm, and the total number of cells is 1.71×10^6. In our simulation, the implicit unsteady solver is used, and the time iteration step is 0.001 seconds. In order to ensure that the residual is within an allowable range, the maximum number of internal iteration steps is set to 5.
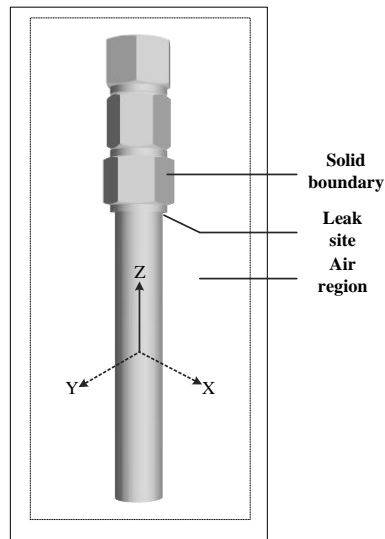
a. Computational domain for the vertical capped

fitting configuration.
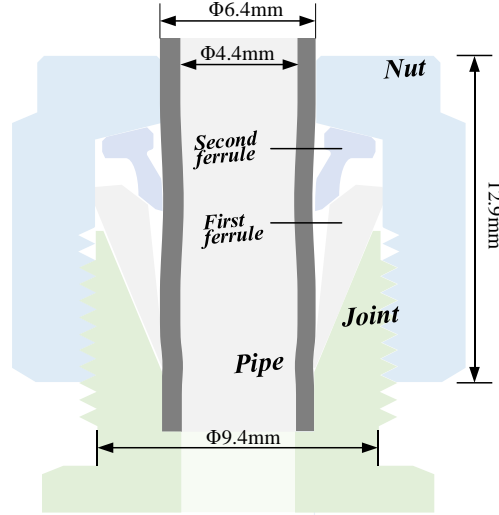
b. Sectional view of the double ferrule joint.
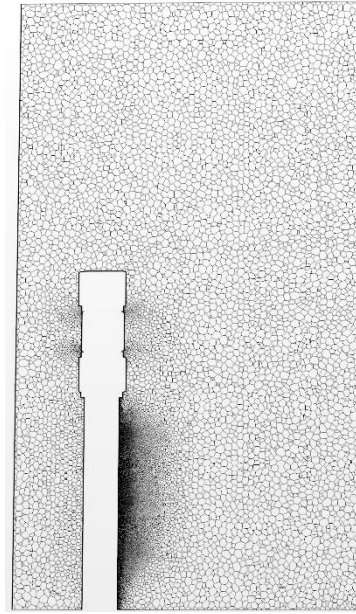
c. computational mesh.

Fig. 1 Computational domain (a. Domain size: L×W×H = 20×20×40 cm), sectional view of the double ferrule

joint, and computational mesh (c. cell size range of 40μm –2000μm).

3. Experimental measurements

Four failure modes of double ferrule joint are considered in this study, namely, 1) The pipe is scratched or flattened, 2) The nut tightening force is insufficient, 3) The double ferrule is flattened or broken, and 4) Foreign matter. The leakage positions of the ferrule corresponding to the four modes are mainly concentrated at the rear end of the nut (REN) and the thread outlet (TO). For mode 1) and mode 4), it usually only leaks at the rear end of the nut, while for mode 2) and mode 3), it usually leaks on both sides.
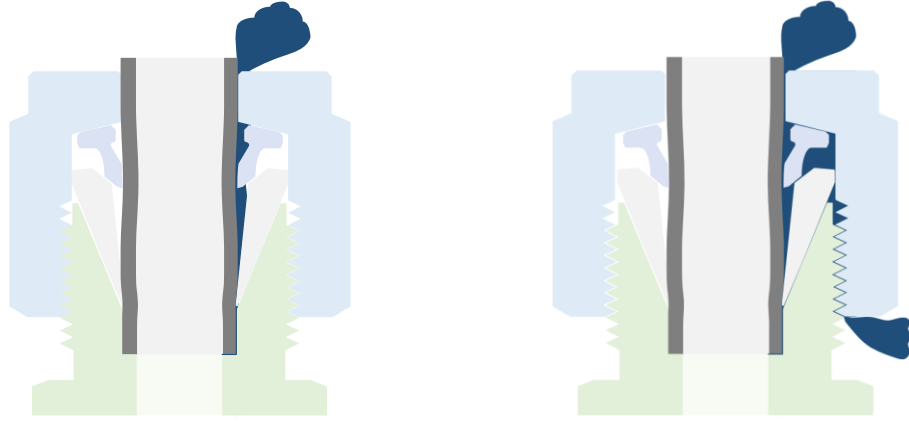
a. Leakage positions at the rear end of the nut   **b.** Leakage positions at the thread outlet and rear end

Fig. 2 Common leakage positions of double ferrule joint

Fig. 3 hydrogen tube leakage test bench.

Experiments were performed in a hydrogen pipework leakage test bench, as shown in **Fig. 3**. High-pressure hydrogen will leak from the control tube to the flawed double ferrule joint. Taking into account the pressure and flow range commonly used in the hydrogen supply pipe of fuel cell vehicles, the pressure and flow adjustment range is 0~2 MPa and 0~5 SLPM. The images of the leaking hydrogen were captured by a high-speed camera (Photron NOVA S16) at a frequency of 12800 Hz (1024 × 1024). The schlieren system is used to image hydrogen, and its effective observation area is Φ =200mm.

We found 50 samples with scratches from the eliminated hydrogen pipeworks for vehicles and observed them under SEM. These 50 pipelines are the defective pipelines found in the FCV's hydrogen storage system. Some of them have been used in the car and have been replaced due to leakage, and some of them have passed the air tightness inspection before leaving the factory. The leak found. **Fig. 4** shows a representative SEM image of pipe scratches in the sample. It can be seen that the scratches are mainly arcs and extend along the axial direction. Statistics on the width of the scratches show that the range of the scratches is 57.1-357.9 μm, and the concentrated width range is between 57-150 μm. In the subsequent design of defective pipes, rectangular scratches will be designed within the range between 500-750 μm. Taking into account that there may be more severe scratches than the above statistical conclusions in real application scenarios, we designed two specifications of scratches for 1/4 stainless steel pipes, as shown in **Table 1**. The sizes of the scratches are 500×500 μm and 750×750 μm, and their actual pictures are shown in the right column of **Table 1** (scratch shown in the red frame).
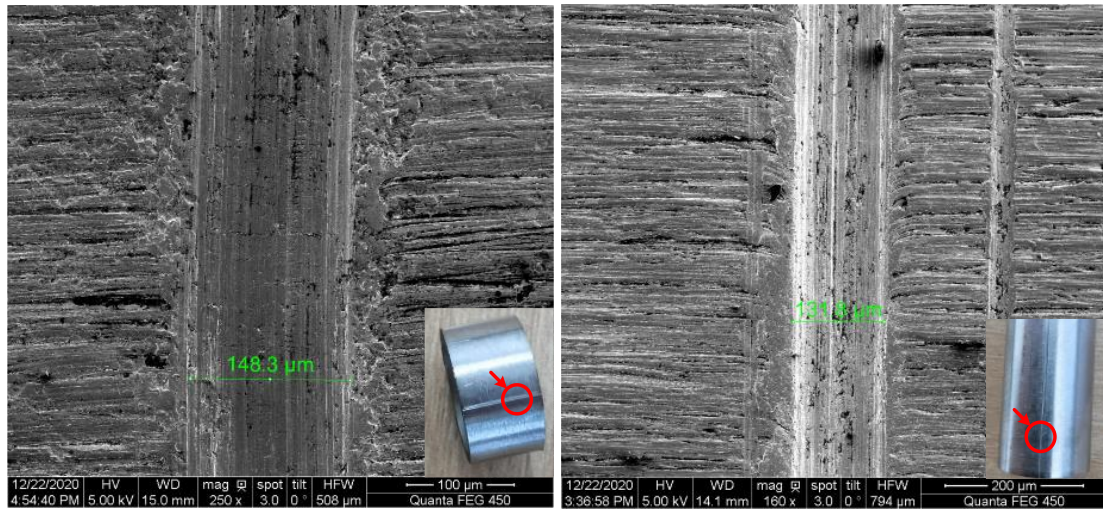
a. Scratched sample A　　　　　　　　　**b**. Scratched sample B

Fig. 4 Surface SEM images of cell Scratched tube.

Table 1 Designed three specifications of scratches

Scratch Sample	Size of the scratch (μm)	Description
Small scratches (SS)	500×500	
Mesoscale scratches (MS)	750×750	

4.　Results and discussion

Hydrogen leaks from the rear end of the nut – scratch leakage

The physical conditions and geometric shapes of the numerical simulation are reproduced by the fluid calculation software, and the calculated CFD model is compared with the experiment in the vertical and horizontal directions. **Fig. 5** shows the hydrogen leakage morphology, the concentration range is 4%-100% mol/mol, and the leakage velocity is 100m/s. In the vertical downward jet process, the jet direction is opposite to the buoyancy direction, and the hydrogen-air mixture will locally accumulate and further increase the turbulence. Therefore, the volume of the combustible area will be larger than that of the horizontally leaking jet. From the perspective of the cross-sectional view, when a scratch leak occurs, hydrogen will diffuse quickly. This is mainly because the scratch leak is a small amount of leakage and has begun to diffuse at the leak outlet. Therefore, it can be seen in the cross-sectional view that most of the diffusion area has a very low concentration, and even the concentration at the leakage outlet is not high. The fitting concentration profile of the model corresponded qualitatively to the schlieren images taken from the same perspective.

Fig. 6 shows the gas flow morphology of hydrogen leakage when there is a longitudinal scratch. The depth of the scratch is 0.75 mm and the width is 0.75 mm. In the experiment, in addition to the pressure reducing valve to control the released initial pressure, a needle valve was installed at the end of the leak outlet. The needle valve further controls the leakage flow. When the needle valve is fully opened, the leakage will be open released with the initial pressure. The "Inf" represents open leakage at the current initial pressure. When a small flow rate is leaked (less than 2 SLPM), the leaked hydrogen is mainly in the form of laminar diffusion, which will go down in the direction of the jet. From the perspective of the airflow boundary, the gas flow is also affected by the external air, and fluctuates with the flow of the environment during the ascent. When the flow rate exceeds 2SLPM, the hydrogen jet changes from laminar flow to turbulent flow, and it couples with the surrounding environment to generate vortices. At the same time, the jet is affected by the boundary layer on the pipe, and the jet no longer stays on the side close to the scratch, but spreads around the pipe.
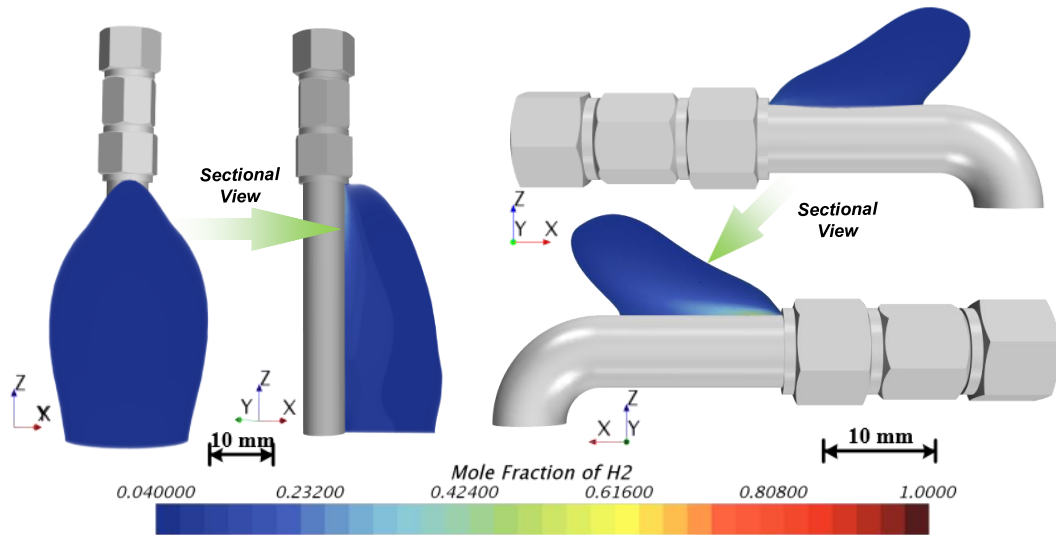
Fig. 5 The isosurface of 4% hydrogen mole fraction when leaking at the rear end of the nut. Vertical and horizontal
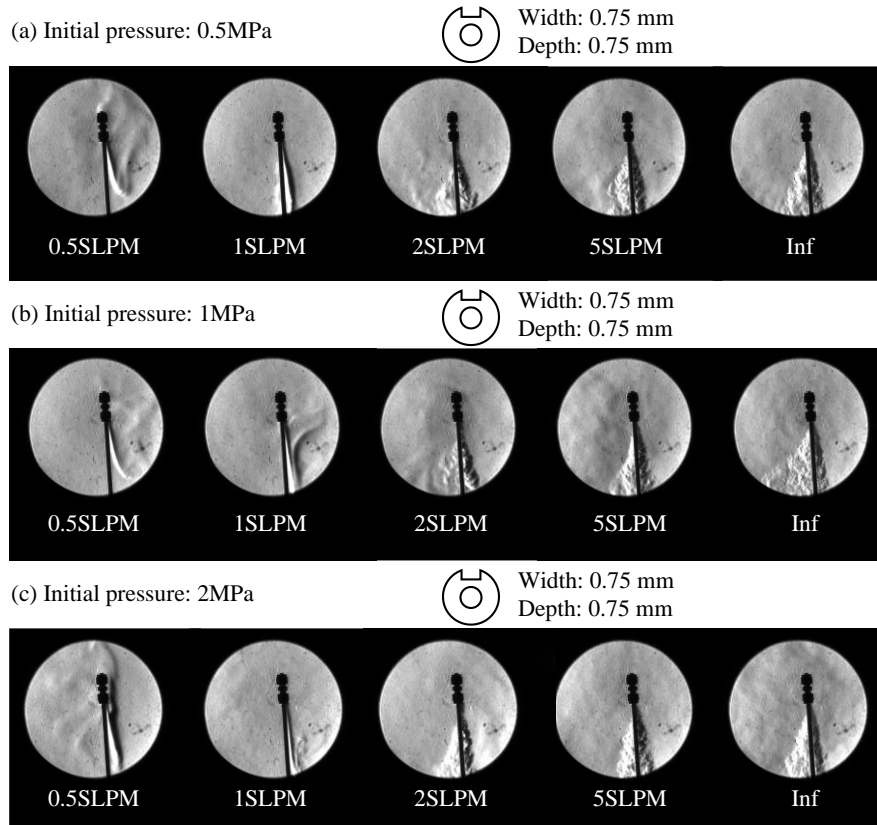
assembly direction.

Fig. 6 Transmission schlieren images of the vertical oriented fitting leakage with the scratch size: width: 0.75

mm/Depth: 0.75 mm. (a) Release pressure: 0.5MPa; (b) Release pressure: 1MPa; (c) Release pressure: 2MPa.
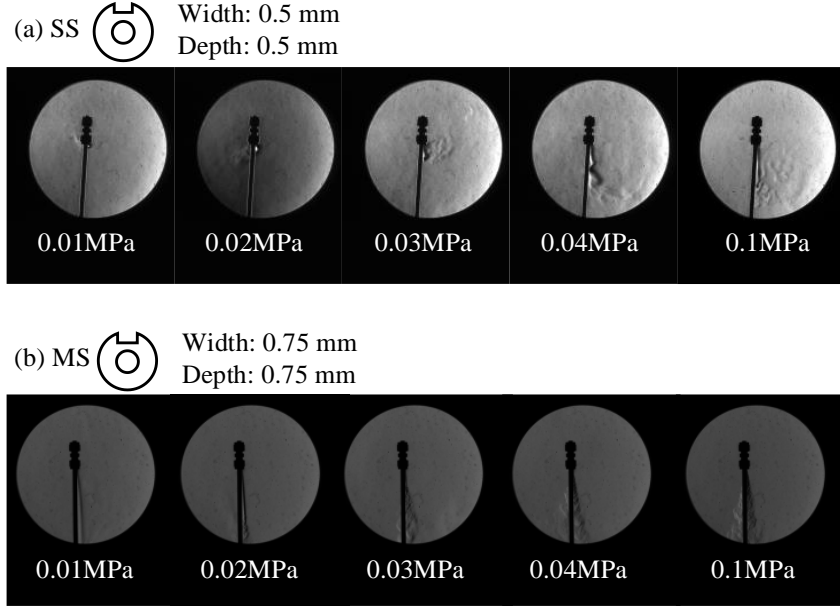
Fig. 7 Transmission schlieren images of the vertical oriented fitting leakage in different pressure with the scratch size: (a) SS, (b) MS.
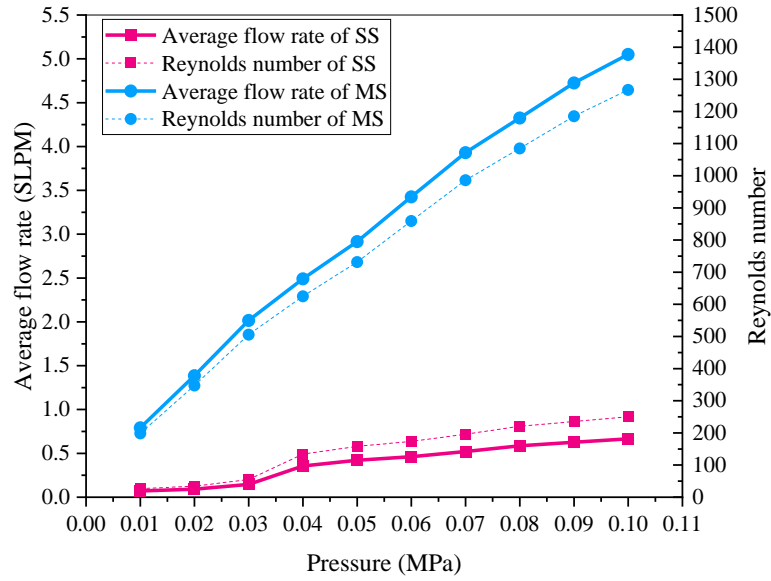
Fig. 8 Average flow rate and Reynolds number in three types of scratches with different pressure.

Fig. 7 shows the leakage schlieren images of the two types of scratches that gradually increase with the relief pressure. For SS leakage mode, before the discharge pressure is less than 0.1 MPa, the leakage flow is less than 1 SLPM. At this time, the gas from the jet is mainly affected by buoyancy and background flow and appears floating and swaying. When the leakage pressure reaches 0.1MPa, the initial momentum gradually increases, and the jet morphology begins to form.

For the MS leakage mode, the initial momentum dominates in the schlieren observation window, forming laminar jets and turbulent jets. Under the maximum leakage pressure of 0.1MPa, the leakage flow and Reynolds number are 5.05SLPM and 1267, respectively. The measured leakage flow rate and the calculated Reynolds number are shown in **Fig. 8**. For MS leakage, the observed Reynolds number (505 in 0.03MPa) corresponding to the observed laminar-turbulent transition is much smaller than the lower critical Reynolds number (about 2000). This is mainly due to the complexity of the leakage scenario (the presence of pipe obstacles in the leakage path), and the impact of environmental disturbances that cause turbulence to appear at low initial pressures (0.03MPa).

Hydrogen leaks from the rear end of the nut and thread outlet on the double tube joint

The geometric shape, physical conditions, and boundary conditions are reproduced by numerical simulation, and the CFD model is compared with the experiment of the leakage at the rear end of the nut and thread outlet. **Fig. 9** shows the solution of the Realizable Two-Layer K-ε model attached to the RANS model. The simulated leakage flow rate is 5 SLPM. And use the 30% hydrogen volume fraction boundary is shown in **Fig. 9** is used to represent the observed gas flow morphology.

Fig. 10 shows the changes in the volume of hydrogen enveloped by different mole fraction values over time. The leakage method at this time is at the rear end of the nut and thread outlet, and the leakage direction is horizontal assembly direction. It can be seen that the volume of hydrogen higher than 20% mol/mol will not change with time, and the main change range is 1%-20% mol/mol. When the leakage flow rate of 5 SLPM leaks for 3 seconds, the envelope volume of 1% mol/mol is 8.7 L, and the envelope volume of 4 %mol/mol is 3.18 L.
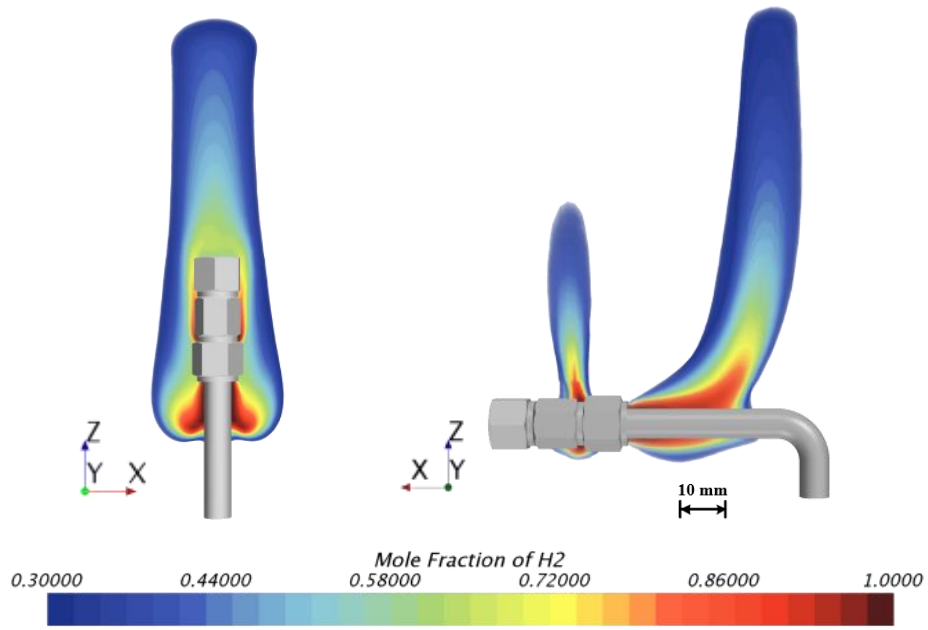
Fig. 9 Simulation of hydrogen mole fraction when leaking at the rear end of the nut and thread outlet. Vertical and horizontal assembly direction.
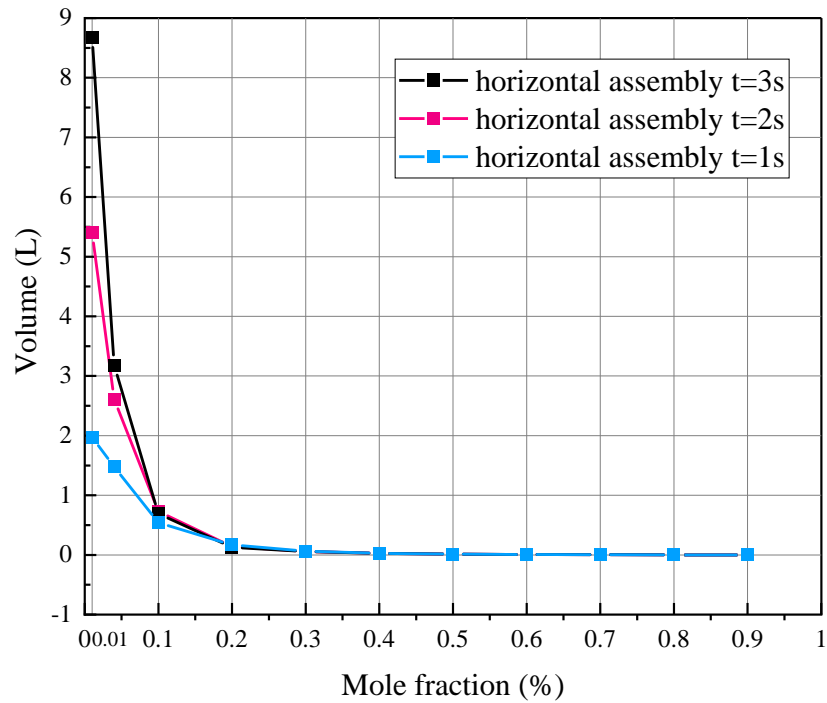

Fig. 10 The change of the volume of hydrogen with different mole fractions over time. Leakage at the rear end of the nut and thread outlet. Horizontal assembly direction.

5. Conclusions

This paper analyzes the four failure modes of double ferrule joints commonly used in hydrogen systems. Under the four failure modes, there are two main forms of leakage, namely leakage positions at the rear end of the nut and leakage positions at the thread outlet and rear end. We believe that the leakage from the rear end of the nut will always occur when the four types of failure modes happen. For the two leakage forms, the schlieren method was used for observation and CFD was used for simulation. In the case of scratch leakage, a statistical analysis of scratch size is carried out, and three scratch sizes are given based on the statistical results. For the two scratch sizes, we found that the critical pressure values for the vortex transition observed in the laminar flow direction are 0.2 MPa and 0.03 MPa. A numerical model is used to study the influence of the hydrogen flow rate on the concentration field distribution of the hydrogen-air mixture under the scenario of a scratched pipe and a leak on both sides of the nut. We found that for the numerical simulation of the leakage caused by scratches, the numerical simulation of the leakage morphology and the observed morphology are in good agreement with the small flow leakage (less than 2 SLPM). Through our experiments, some practical applications and suggestions can be given:

1. When we conducted the statistics of defective pipelines, in addition to the scratches along the axial direction, some " concavities" were also found on the surface of the steel pipe. The shape of " concavities" is mostly elliptical, which is an inward collapse caused by the collision of steel pipes. If these "concavities" are positioned in the sealing area between the steel pipe and the double ferrule, the sealing effect of the double ferrule will fail. Therefore, the surface inspection of the stainless steel pipe in the pipeline assembly becomes very important.

2. In the four failure modes, leakage from the rear of the nut is inevitable. This is because there is a gap between the nut and the steel pipe. Therefore, it is feasible to develop a sensor that can quickly detect leakage at the end of the joint.

3. In the actual hydrogen system pipeline, the scratch width ranges from 57.1 to 357.9 μm. Therefore, SS is closer to the actual environment. When the internal pressure of the hydrogen system reaches 0.1 MPa, the hydrogen flow rate due to scratch leakage is about 1 SLPM. Therefore, in the hydrogen system leak detection, the detection of the pipe joints one by one becomes very important, and the detector is required to have higher detection accuracy.

However, for large-flow leakage, the numerical simulation results failed to obtain a tail-like leakage morphology bypassing the leaking pipework, which is contrary to the experimental observation results. The reasons may be: 1) The fluid parameter setting is improper; 2) The interface setting in the simulation is unreasonable. It needs to be further improved in the simulation accuracy. Besides, the high-pressure leakage morphology of the pipe and the possibility of spontaneous ignition due to leakage collision would be the next step in a future study.

References:

[1] G. Jirka, Integral model for turbulent buoyant jets in unbounded stratified flows. Part 2: Plane jet dynamics resulting from multiport diffuser jets, ENVIRON FLUID MECH, 6 (2006) 43-100.

[2] G.H. Jirka, Integral Model for Turbulent Buoyant Jets in Unbounded Stratified Flows. Part I: Single Round Jet, ENVIRON FLUID MECH, 4 (2004) 1-56.

[3] J. Kim, W. Yang, Y. Kim, S. Won, Behavior of buoyancy and momentum controlled hydrogen jets and flames emitted into the quiescent atmosphere, J LOSS PREVENT PROC, 22 (2009) 943-949.

[4] A.D. Birch, D.J. Hughes, F. Swaffield, Velocity Decay of High Pressure Jets, Combustion Science & Technology, 52 (1987) 161-171.

[5] R.W. Schefer, W.G. Houf, T.C. Williams, B. Bourne, J. Colton, Characterization of high-pressure, underexpanded hydrogen-jet flames, INT J HYDROGEN ENERG, 32 (2007) 2081-2093.

[6] T. Mogi, Y. Wada, Y. Ogata, A.K. Hayashi, Self-ignition and flame propagation of high-pressure hydrogen jet during sudden discharge from a pipe, INT J HYDROGEN ENERG, 34 (2009) 5810-5816.

[7] T. Mogi, D. Kim, H. Shiina, S. Horiguchi, Self-ignition and explosion during discharge of high-pressure hydrogen, J LOSS PREVENT PROC, 21 (2008) 199-204.

[8] V. Gamezo, T. Ogawa, E. Oran, Flame acceleration and DDT in channels with obstacles: Effect of obstacle spacing, COMBUST FLAME, 155 (2008) 302-315.

[9] W. Han, Y. Gao, C. Law, Flame acceleration and deflagration-to-detonation transition in micro and macro-channels: An integrated mechanistic study, COMBUST FLAME, 176 (2017) 285-298.

[10] E.G. Merilo, M.A. Groethe, R.C. Adamo, R.W. Schefer, W.G. Houf, D.E. Dedrick, Self-ignition of hydrogen releases through electrostatic discharge induced by entrained particulates, INT J HYDROGEN ENERG, 37 (2012) 17561-17570.

[11] M. Glor, Ignition hazard due to static electricity in particulate processes, POWDER TECHNOL, 135 (2003) 223-233.

[12] T. Imamura, T. Mogi, Y. Wada, Control of the ignition possibility of hydrogen by electrostatic discharge at a ventilation duct outlet, INT J HYDROGEN ENERG, 34 (2009) 2815-2823.

[13] R. Ono, M. Nifuku, S. Fujiwara, S. Horiguchi, T. Oda, Minimum ignition energy of hydrogen–air mixture: Effects of humidity and spark duration, J ELECTROSTAT, 65 (2007) 87-93.

[14] K. Nasrifar, Comparative study of eleven equations of state in predicting the thermodynamic properties of hydrogen, INT J HYDROGEN ENERG, 35 (2010) 3802-3811.

[15] G. Ernst, B. Keil, H. Wirbser, M. Jaeschke, Flow-calorimetric results for the massic heat capacitycpand the Joule–Thomson coefficient of CH4, of (0.85CH4 + 0.15C2H6), and of a mixture similar to natural gas, J CHEM THERMODYN, 33 (2001) 601-613.

[16] T. Mogi, Y. Wada, Y. Ogata, A.K. Hayashi, Self-ignition and flame propagation of high-pressure hydrogen jet during sudden discharge from a pipe, INT J HYDROGEN ENERG, 34 (2009) 5810-5816.

[17] P. Cho, C.K. Law, Catalytic ignition of fuel/oxygen/nitrogen mixtures over platinum, COMBUST FLAME, 66 (1986) 159-170.

[18] N. Rubtsov, V. Chernysh, G. Tsvetkov, K. Troshin, I. Shamshin, Ignition of hydrogen-methane-air mixtures over Pd foil at atmospheric pressure, MENDELEEV COMMUN, 29 (2019) 469-471.

[19] A. Ungut, H. James, Autoignition of gaseous fuel-air mixtures near a hot surface, RUGBY, 2001. pp. 487-501.

[20] D. Brearley, P. Tolson, The frictional ignition properties of (18/8) stainless steel, HSL internal report no.IR/L/IC/95/02, (1995).

[21] P. Li, Q. Duan, L. Gong, K. Jin, J. Chen, J. Sun, Effects of obstacles inside the tube on the shock wave propagation and spontaneous ignition of high-pressure hydrogen, FUEL, 236 (2019) 1586-1594.

[22] Q. Duan, H. Xiao, W. Gao, L. Gong, J. Sun, Experimental investigation of spontaneous ignition and flame propagation at pressurized hydrogen release through tubes with varying cross-section, J HAZARD MATER, 320 (2016) 18-26.

[23] T. Shih, W.W. Liou, A. Shabbir, Z. Yang, J. Zhu, A new k-ϵ eddy viscosity model for high reynolds number turbulent flows, COMPUT FLUIDS, 24 (1995) 227-238.

[24] RODI, W., Experience with two-layer models combining the k-epsilon model with a one-equation model near the wall, 29th AIAA Aerospace Sciences Meeting, (1991).

[25] A. Obieglo, J. Gass, D. Poulikakos, Comparative study of modeling a hydrogen nonpremixed turbulent flame, COMBUST FLAME, 122 (2000) 176-194.

[26] W.G. Houf, G.H. Evans, R.W. Schefer, Analysis of jet flames and unignited jets from unintended releases of hydrogen ☆, INT J HYDROGEN ENERG, 34 (2009) 5961-5969.

[27] V. Molkov, V. Shentsov, S. Brennan, D. Makarov, Hydrogen non-premixed combustion in enclosure with one vent and sustained release: Numerical experiments, INT J HYDROGEN ENERG, 39 (2014) 10788-10801.

Responses to Reviewers' comments#1

Comment 1: AUTHOR COMMENTS: There are some sentences in the introduction where the use of English is unconventional or the statements seem unusual or need further clarification. As a first example, you say:

"For any accident caused by hydrogen spontaneous ignition, the underlying mechanism is complicated, because the occurrence of accidents is usually the result of a combination of multiple theories."

Do you mean to say something like "The cause of ignition is often uncertain in accidents involving ignited hydrogen releases"?

Response: Thank you for your comment. The original intention is that for any spontaneous combustion accident that occurs in reality, the underlying cause is the superposition of multiple spontaneous combustion theories. We further polished the sentence structure. As follows:

For any accident caused by the spontaneous combustion of hydrogen, the potential spontaneous combustion mechanism is complicated, because this spontaneous combustion is often the result of the superposition of multiple theories.

Comment 2: And a second example:

"Hydrogen spontaneous ignition caused by static electricity is currently the most speculated cause of ignition."

Do you mean to say something like: "Electrostatic ignition is often cited as the most likely cause of unexplained ignitions of hydrogen."?

Response: Thank you for your comment, yes, the meaning in the manuscript is as you said, we further polished the sentence.

Comment 3: As a third example, the paper talks about "pipelines" but I think you are you talking about "pipework". The term "pipeline" mainly refers to large diameter pipes (usually buried in the ground) that transport gases and liquids over large distances (on the scale of kilometres). Pipework is the collective term used for (usually) smaller diameter pipes in plant rooms, vehicles etc.

Response: Thank you for your comment. In fact, our research is only aimed at a pipe connection method, that is, a double ferrule joint connection method. So as to the difference between "pipeline" and "pipework" you mentioned, as long as the connection method of double ferrule joint is used, our analysis is applicable. Thank you for your reminder. We have replaced the "pipeline" in the full text as appropriate.

Comment 4: In Figure 1b, please could you add some dimensions to the cross-section of the joint to give the reader an impression of the scale?

Response: Thank you for your comment. According to your suggestion, we have marked the key size information in the Figure 1b.

Comment5: "The LES separates large-scale vortices from small-scale vortices through a filter function.

Large-scale vortices are directly numerically simulated, and small-scale vortices are closed by models. To solve the key turbulence structure near the wall, this method requires a higher grid resolution in the wall boundary layer, which is not only reflected in the direction perpendicular to the wall but also in the flow direction. DES is a hybrid modeling method that combines the high resolution of the large eddy simulation method in the separated flow region and the high efficiency of the Reynolds average method in the attached boundary layer[24]."

The modelling study presented in the paper has used RANS, not LES. Therefore, this paragraph could be removed without losing anything from the paper.

Response: Thanks for your comment. Based on your suggestion, we have deleted the description of LES.

Comment 6: Was the thermal radiation model used in the CFD simulations? If not, then the section describing the radiation model could also be removed.

Response: Thank you for your comment. The thermal radiation model has been added to the simulation. Although its impact is extremely small, in order to ensure the accuracy of the simulation, we hope to make the model as accurate as possible.

Comment 7: "The temperature of the hydrogen leaking from the pipeline is 273 K". Please could you explain why the hydrogen was colder than ambient?

Response: Thank you for your comment. The reason for setting the hydrogen temperature to 273K and the ambient air temperature to 293K is to study the temperature changes in different concentration areas of hydrogen-air mixture during the jetting process. That is, the dynamic process of heating up to ambient temperature after the leakage of low-temperature hydrogen. We consider that this paper does not involve the issue of combustion after leakage, so this manuscript does not analyze the heating process. This will also be one of the focuses of our follow-up research. Thanks again for your comment.

Comment 8: One of the challenges with running CFD simulations for this case is the very small size of the leakage paths (tens of microns) when the scales of the dispersion in the surrounding atmosphere are much larger (tens of centimetres). Please could you explain how many cells were used to span the width of the crack inside the pipe fitting? And whether any tests have been undertaken to assess the sensitivity of the results to the grid resolution?

Response: Thank you for your comment. We have further explained some key parameters in the article. We have expanded the cell size setting range, and the minimum cell size is 40 microns to meet the small size (0.5mm) grid division at the scratch. The maximum size is 2000 microns, which takes into account the compromise in the calculation time, and the uniform transition from the

scratch to the environment, so as to ensure that the grid calculation is reasonable. We verified the independence of the cell. Changing the cell size can ensure that the calculation is convergent, and at the same time, it has little effect on the calculation results.

Comment 9: "This paper focuses on the double ferrule joint used in the hydrogen pipeline and presents the
diffusion form and flame shape in six failure modes of the double ferrule joint. The schlieren and high-speed camera is used to observe the hydrogen diffusion morphology. The morphology defects were observed by scanning electron microscope (SEM). Further, the commercial computational fluid dynamics (CFD) software STAR-CCM+ V13.04 produced by CD-adapco was used to simulate the diffusion form and flame shape."
"The flame images of the leaking hydrogen were captured by a high-speed camera."
When you say "flame" it implies the hydrogen was ignited. Please could you clarify? Are the gas releases ignited in the experiments and Schlieren images, but the CFD results show unignited gas dispersion results? This is an important point.

Response: Thank you for pointing out the problem. In fact, we want to add the leak ignition related test of the pipe joint, but due to the urgency of time, we could not add the ignition content, so some problems appeared in the writing. Thanks for your comment, this question has been revised in the full text.

Comment 10: "We found 50 samples with scratches from the eliminated hydrogen pipelines for vehicles."
Please could you clarify? Have you obtained 50 samples of pipework that were found to leak from hydrogen vehicles? Or from hydrogen vehicle refuelling stations?

Response: Thank you for your comment. These 50 pipelines are defective pipelines found in the FCV's hydrogen storage system. Some of them have been used in the car and have been replaced due to leakage, and some have passed before leaving the factory. Due to its small molecular volume, hydrogen is prone to leaks. The 50 defective pipelines come from visual inspection of scratches on the one hand, and leaks detected by the leak detector on the other hand.

Comment 11: Please could you annotate the diagrams shown in the right column in Table 1? It is unclear what the diagrams show.

Response: Thank you for your comment. Table 1 has been re-annotated and explained in the manuscript.

Comment 12: "Fig. 5 shows the 4% mole fractional isosurface when the leakage flow is 100m/s."
Please could you clarify? The coloured contours in the figure show the mole fraction of hydrogen in the range from the lower flammability limit of 4% mol/mol to 100% mol/mol. Please could you

say in the figure caption that a logarithmic scale has been used for the colours (I think this is the case, but it is not immediately obvious)? Could you explain why did you picked a logarithmic colour scale instead of a linear scale, since as a consequence the contour colour is nearly all blue? Is the shape of the surface defined by a velocity of 100 m/s? If so, please could you explain in the text why you decided to show the contours on an iso-surface of velocity?

Response: First of all, the concentration range of the hydrogen leakage profile shown in Figure 5 is 4%-100% mol/mol, and the leakage outlet velocity is 100m/s. Secondly, Figure 5 uses a linear contour color scale instead of a logarithmic contour color scale. We have modified Figure 5 and also reinterpret Figure 5 to avoid readers' misunderstanding. Finally, the outer contour of the leakage flow field is a 4% mole fraction isosurface. The reason why the interior is basically blue is that the leakage flow is small, and the diffusion effect is dominant at this time, so the high concentration area is almost invisible.

Comment 13: These plots in Figure 5 are compared to the Schlieren images in Figure 6, which are cross-sections through the flow, rather than iso-surfaces of velocity. Would it be possible to produce cross-sections of the CFD results to enable like-for-like comparisons to the Schlieren images?

Response: Thank you for your comment. In fact, Figure 5 contains two cross-sectional views. In the latest manuscript, we have further explained in Figure 5.

Comment 14: Figure 9 shows similar CFD results for the second release scenario, but it uses a contour colour scale that is linear (not logarithmic) which varies between 30% and 100% mol/mol. Please could you use the same contour colour scales in Figures 5 and 9 to allow the two plots to be compared?

Response: Thank you for your comment. In fact, Figure 5 and Figure 9 use the same contour color scale. The difference is that the color of the contour color scale in Figure 5 is gradual. But the color of the contour color scale in Figure 9 is discrete. Both of them are all linear rather than logarithmic changes. In order to avoid confusion, we have unified the contour color scales in Figure 5 and Figure 9.

Comment 15: One of the key questions of interest from a safety perspective is the size of the flammable cloud produced by these releases? Would it be possible to determine the size of the flammable cloud from your CFD results for a range of pressures or flow rates (in terms of cloud volume and maximum extent of the flammable cloud from the leak location)?

Response: Thank you for your comment. Using our CFD model can give a flammable hydrogen cloud that evolves over time. When considering the evolution of the hydrogen cloud, it is essential to further expand the calculation area. However, when the calculation area is further expanded, the calculation load and calculation accuracy will be greatly challenged. Therefore, when continuing to expand the calculation area, the focus point will be on the hydrogen diffusion characteristics, which will deviate from the focus of this manuscript. We show the changes in the concentration area of hydrogen cloud over time when a bilateral leakage occurs and the placement direction is horizontal,

as shown in Figure 10.

Comment 16: How do these flammable cloud extents compare to zoning distances given in hazardous area classification guidance?

This would be very useful practical information that would be of interest to many readers.

Response: Thank you for your comment. In our experiment, when the stagnation pressure is 0.1MPa and the leakage area is 0.75mm×0.75mm, the leakage flow rate has reached 5 SLPM, and the jet effect becomes extremely obvious. At the same time, the sound of the jet was heard during the leak. However, due to the limitation of the diameter of our schlieren mirror, the complete leakage morphology cannot be observed. This jet length will also be the focus of our follow-up research. Thanks again for your comment.

credible.

Responses to Reviewers' comments#2

Comment 1: AUTHOR COMMENTS: The study aims at numerical simulations to characterise potential leakages from hydrogen pipeline fittings. The reviewer has the following suggestions to improve the text and exposition:
- Abstract: 1) please correct "Leakages of hydrogen pipeline are…". 2) Could be beneficial to say that Schlieren+high speed camera are used in experiments, to highlight that the paper covers as well comparison of simulations with experiments. 3) Please complete sentence "In addition, statistical analysis of the morphology and size of the scratches in the pipeline." with a verb to complete its meaning.

Response: Thank you for your comment. We have revised the sentences in the *Abstract* section.

Comment 2: - Not sure highlights are needed in this template for ICHS
- Page 1: not sure it can be said that "all" hydrogen safety incidents starts from leakage and diffusion, but it is more realistic to say that most of the incidents initiates from leakage.

Response: Thanks for your comment, this absolute statement has been revised in the latest manuscript.

Comment 3: - Page 3: Experimental apparatus should not be the title of the chapter where you first describe the numerical model.

Response: Thank you for your comment. We have deleted the *"Experimental apparatus"* of the page 3.

Comment 4: - Page 4: it is given reference to a Nomenclature section which is not present in the paper.

Response: Thank you for your comment. We re-organized the conservation equations used in CFD calculations and explained the meaning of the variables.

Comment 5: - Page 4: second to last line, please correct to "compared to..."

Response: Thanks for your comment, we corrected this grammatical error.

Comment 6: - Page 5: Eq. 7. Can you describe how convective heat transfer coefficient is determined by the code?

Response: Thank you for your comment. We noticed that in our simulation, there is no interface relationship between the flow field area and the solid area of the pipe joint. Therefore, there is no convective heat transfer, and we deleted the model introduction of this heat transfer part. In Starccm+, the convective heat transfer coefficient is defined by setting the heat flow at the interface.

Comment 7: - Page 5: you can split sentence between Eq.8 and Eq.9 into two sentences: "…Boltzmann constant. When…"

Response: Thanks for the comment. In accordance with your comments, we have revised the sentence structure.

Comment 8: - Page 6: Fig1a please correct boundry to boundary

Response: Thanks for your comment, we corrected this wrong word.

Comment 9: - Page 6 line 4, possibly a pronoun is missing.

Response: Thank you for your comment. We have revised this sentence and polished the writing of the full manuscript.

Comment 10: - Figure 5: what does Inf stands for? A reader may think that it stands for infinite, but it would note really match with the indication of flow rate in other sub-figures.

Response: Thank you for your comment. "Inf" in Figure 6 stands for "infinite". In our experiment, in addition to the pressure reducing valve to control the released stagnation pressure, we installed a needle valve at the end of the leak outlet. The needle valve further controls the leakage flow. When the needle valve is fully opened, the leakage will be open released with stagnation pressure. For the "Inf" in the Figure 6, we have made a further explanation in the original text.

Comment 11: The reviewer has the following comments and questions:
could you please add information about the time discretization?

Response: Thanks for the comment. In our simulation, the Implicit Unsteady Solver is used, and the time iteration step is 0.001 seconds. In order to ensure that the residual is within an allowable range, the maximum number of internal iteration steps is set to 5. We have further explained this in the manuscript.

Comment 12: have you conducted any time step and grid sensitivity analyses? Could you please add information about them or reasoning why these were not conducted yet.

Response: Thanks for your comment, we performed a sensitivity analysis for calculating the time step and cell size. The variation range of the system residuals caused by parameter sensitivity is not obvious, and the system residuals can be guaranteed to be below 10^{-3}. Therefore, the accuracy of the simulation can be guaranteed.

Comment 13: would it be possible to obtain from conclusions some practical applications and suggestions to avoid the mentioned hazardous scenarios?

Response: Thanks for your comments, we will further elaborate some suggestions in the summary,

Comment 14: it would be useful to add space and dimensions in the figures of hydrogen distributions to understand what is the extent of the hydrogen flammable mixtures in the surroundings of the fittings.

Response: Thanks for the comments. Based on the comments, we have added a scale in Figure 5 and Figure 9 to help readers have an intuitive understanding.

Comment 15: conclusions justify the disagreement between simulations and experiments for large flow leakages by the following reasons: "1) The fluid parameter setting is improper; 2) The interface setting in the simulation is unreasonable." Would not these two factors be common to low flow leakages and therefore deeply affect and interfere with accuracy of their simulations too? Please clarify this aspect.

Response: Thanks for the comments. In our work, the simulation results for the laminar diffusion process can correspond well with the experimental results before critical pressure values for the transition. However, we cannot simulate the "umbrella" jet after the critical pressure values through set the key parameters. We conclude that there are two main reasons for simulation inaccuracy: 1) The fluid parameter setting is improper, and 2) The interface setting in the simulation is unreasonable.

For the simulation results of low flow leakage, we can ensure that the parameter setting is reasonable, the system residuals can be guaranteed to be below 10^{-3}. The influence of interface setting in this time is small. Therefore, we believe that the low flow leakage simulation results are credible.